Rubber-Modified Glassy Amorphous Polymers Prepared via Chemically Induced Phase Separation. 1. Morphology Development and Mechanical Properties

B. J. P. Jansen, S. Rastogi, H. E. H. Meijer,* and P. J. Lemstra

Eindhoven Polymer Laboratories, The Dutch Polymer Institute, Eindhoven University of Technology, PO Box 513, 5600 MB, Eindhoven, The Netherlands

Received October 19, 2000

ABSTRACT: Toughness enhancement of brittle amorphous polymers can be obtained via microstructural adjustments, resulting effectively in a removal of intrinsic strain softening on the mesoscale via a decrease in yield stress and an increase in strain hardening. Generally the introduction of a dispersed soft phase is required with an optimum size that tends to be in the range of several tens of nanometers rather than microns. This morphology cannot be realized via conventional processing techniques like physical blending, and in this study, chemically induced phase separation is used as a route for obtaining a fine dispersion of rubbery particles in polystyrene (PS) and poly(methyl methacrylate) (PMMA). In the case of simultaneously polymerized MMA/aliphatic-epoxy systems tensile toughening is observed at moderate (rubbery) epoxy volume fractions during slow speed deformation. Once the deformation speed is increased to impact conditions, the material, however, responds again in a brittle manner. The observations have been that predeformation of the samples at a low deformation rate, prior to impact testing, precavitates the specimens and regenerates toughness. This indicates that—apart from the obvious influence of the microstructure—the properties of the dispersed phase are of decisive importance.

1. Introduction

1.1. Some Comments on Toughness Improvement. Successful applications of polymeric materials require resistance against mechanical deformation at different loading rates. As a consequence, in the past considerable attention has been paid to reveal the fundamentals of different toughening mechanisms, and especially for amorphous polymers, a vast amount of literature exists concerning rubber toughening and the relation between morphology and both micro- and macroscopic properties; see e.g. the reviews in refs 4 and 5. Although most solutions to toughening problems proved to be quite system specific using systematic modeling on the different relevant length scales involved, recently more general approaches have been proposed.[1−3,6−8] Today it is well established that the brittle nature of polystyrene is the result of catastrophic strain localization in the form of crazes, which causes premature fracture at a relatively small macroscopic deformation. However, within the craze fibrils, very large draw ratios are obtained, indicating that the intrinsic ductility of polystyrene is even higher than that of polycarbonate.[9,10] An apparent difference between these two polymers is their network density, which for polycarbonate results in a higher cavitation stress, less strain softening, more pronounced strain hardening, and a lower maximum network strain.[11,12,15] This results microscopically in less localized deformation in shear bands and, macroscopically, in a higher strain at break in slow speed tensile experiments. Nevertheless, polycarbonate crazes once the test specimen is notched, and brittle behavior results. For this reason, microstructural adjustments are always needed, realized by introducing heterogeneity in polymer systems.[1] Unlike in tensile deformation, in compression neat materials behave rather differently, and the intrinsic network drawability is better reflected.[13] Interestingly, the large strain at break, as measured for e.g. polystyrene in compression, can also be obtained in tensile, albeit mostly via academic, rather than practical, methods. They include methods aiming at a decrease in yield stress (e.g., by the addition of plasticizers or temporarily by fast quenching[14] or mechanical rejuvenation[15]) and alternatively at an increase in hardening modulus (e.g., by cross-linking,[16] preorientation, or rubber toughening[3]). Enhanced mobility could, more practically, be obtained by decreasing the absolute thickness in heterogeneous polymer systems down to the submicron level. The mode of deformation changes from crazing to shear yielding (either by creating sufficiently thin multilayered tapes[17] or by applying high volume fractions of nonadhering core−shell rubber particles[18]), and the macroscopic strain at break approaches the draw ratio observed in craze fibrils. The draw ratio is, accordingly, basically controlled by the maximum network strain. This is called *ultimate toughness*.

The drawback of the most useful system that obtained ultimate toughness, i.e., the polystyrene−rubber blends investigated by van der Sanden et al., is the high amount of rubber (>50 wt % of 200 nm sized core−shell particles) necessary to create the required interparticle distance of about 30 nm. A dispersed phase beyond 50 wt % not only results in a reduced modulus and yield strength of the blend but also could cause problems with the percolation threshold which gives rise to a questionable composition of the continuous phase. Therefore, we performed some additional experiments, using smaller, 80 nm sized, nonadhering core−shell particles that revealed that the critical rubber concentration could be decreased to below 40 wt % (see Figure 1), thus solving the second problem mentioned. Following the trend observed in Figure 1, it would be preferable to introduce (easy cavitating) nanosized (∼30 nm) rubbery dispersions, since they could result in a reduced modulus loss, while maintaining the profitable ductile behavior, since the same critical interparticle distance can be obtained

10.1021/ma001809z CCC: $20.00
Published on Web 05/11/2001

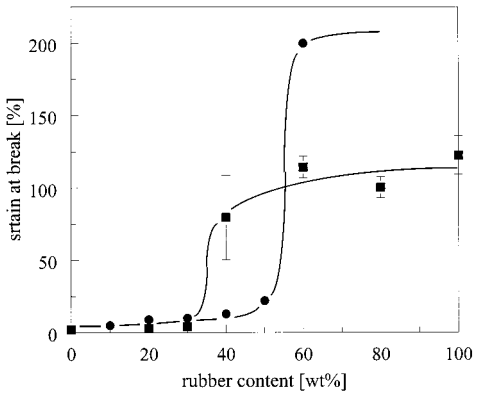

Figure 1. Strain at break vs rubber content of core−shell rubber-modified polystyrene using a particle size of 200 nm (●)[18] and 80 nm (■) (this work).

with much smaller volume fractions, typically <10%. Thus, optically clear, ultimate tough, amorphous polymer systems could result. This is the subject of the present paper.

1.2. CIPS-Based Preparation Techniques. Conventional mechanical blending techniques cannot produce the fine morphologies aimed at. Alternative routes include reactive blending methods, e.g., those where the morphology is a result of a chemically induced phase separation (CIPS) process. Classical examples thereof (that are however obviously not optimal) are the fabrication of high-impact polystyrene (HIPS) and acrylonitrile−butadiene−styrene (ABS)[4] made in situ in the reactor. A second example is the recently developed processing route for intractable, amorphous, high-T_g polymers as introduced by Venderbosch et al. that also involved CIPS processes.[19] In their study, both aromatic and aliphatic epoxy resins were used as reactive solvents for poly(2,6-dimethyl-1,4-phenylene ether) (PPE), resulting in solutions that could be processed at relatively low temperatures. After processing, the PPE/epoxy solutions were cured, and phase separation combined with phase inversion was induced, resulting in blends of dispersed epoxy particles in a thermoplastic PPE matrix. By using aliphatic epoxies, a micron-sized dispersed rubbery phase was obtained, which also improved the mechanical properties of the resulting blend.[20] In contrast to the conclusions of Venderbosch et al. concerning the obtainable size of the dispersed phase, it has been shown that the morphology of the reactive systems could indeed be tailored by adjusting the viscosity of the solution during phase separation.[21] This procedure allows the production of nanosized morphologies in, originally brittle, amorphous polymers like PS and PMMA. Despite this, control over the adhesion between dispersed and continuous phase and/or the easiness of internal cavitation of the dispersed phase are not straightforward issues. In this work, deformation tests at different rates were conducted along with in-situ morphological studies using time-resolved X-ray scattering, to reveal the underlying microscopic deformation processes.[35−37]

2. Experimental Section

2.1. Materials. Two amorphous polymers were used: polystyrene (PS, SHELL N5000, $M_w = 260$ kg/mol) and poly(methyl methacrylate) (PMMA, Atohaas VO52, $M_w = 110$ kg/mol). The epoxy resin is a diglycidyl ether of polypropylene oxide (DGEPPO, SHELL Epikote 877). The curing agent, Jeffamine D230, supplied by Huntsman (Zaventem, Belgium), is a diamine, which is also based on a poly(propylene oxide) (PPO) backbone. The free-radical polymerization of methyl methacrylate (MMA, Aldrich, purified prior to use) was performed over a broad temperature range which required the application of three initiators with different reactivities: 2,2′-azobis(4-methoxy-2,4-dimethylvaleronitrile) (V-70 initiator supplied by WAKO Chemicals, Neuss, Germany), 2,2-azobis(isobutyronitrile) (Perkadox AIBN, AKZO−NOBEL), and *tert*-butyl peroxybenzoate (Aldrich). The half-life time for decomposition of these initiators decreases with increasing temperature from 30, 64, to 103 °C.

2.2. Blend Preparation. Mixtures of PS or PMMA with epoxy resin were prepared using a Brabender Plasticorder kneader. First, two homogeneous solutions of thermoplast with epoxy resin and thermoplast with curing agent were prepared. Subsequently, the two solutions were mixed (to obtain a stoichiometric mixture of epoxy and amine curing agent) at elevated temperatures and short processing times (to prevent premature polymerization and phase separation). Finally, the solutions were compression-molded and cured at various temperatures.

Alternatively, PMMA/epoxy blends were prepared by the simultaneous polymerization of MMA and epoxy via a procedure that maintained control over the coarsening process. Homogeneous solutions of MMA, epoxy, curing agent, and all three free-radical initiators mentioned were prepared at room temperature for several MMA−epoxy weight ratios. The solutions were poured into cast molds, which were closed after being purged with nitrogen gas for several minutes, and kept at room temperature for 24 h during which the free-radical MMA polymerization was initiated by the most reactive initiator, V-70. Accordingly, the molds were placed in an oven with a programmed temperature profile: 20 h at, subsequently, 30, 50, 70, and 90 °C, followed by two postcuring steps at 110 °C for 3 h and 120 °C for 2 h. The three free-radical initiators with different half-life time were applied in order to ensure the continuation of the MMA polymerization over the entire temperature range. After completion of the polymerization, the molds were kept in the oven, which was allowed to cool slowly to room temperature.

2.3. Analysis. A dynamic mechanical thermal analyzer (Rheometrics Scientific, MkII) was used in bending mode (frequency of 1 Hz, strain of 40 μm, and heating rate of 2 °C/min) to investigate the dynamic response, with emphasis on the T_g's, of all the samples. Their morphology was studied using both scanning (SEM, Cambridge Strereoscan 200) and transmission (TEM, JEOL 2000 FX) electron microscopy. (Surfaces of the SEM samples were microtomed at liquid nitrogen temperature, etched with oxygen plasma and coated with gold−palladium layer; the TEM coupes were microtomed on a Reichert-Jung Ultracut E ultratome and stained with RuO_4 vapor for 10 min.) Raman measurements were performed to study the kinetics of the MMA polymerization at 90 °C in the presence of epoxy resin. Spectra were collected using a Dilor XY-800 spectrograph coupled with a liquid nitrogen cooled Princeton CCD array detector. The 488 nm laser line was used to monitor the polymerization reactions which were performed in sealed glass capillaries heated in a Linkham THMS 600 hot stage.

2.4. Mechanical Properties. Tensile tests were performed at room temperature using a Zwick 1445 tensile machine. Dog-bone-shaped tensile bars with a gauge length of 38 mm were machined from the polymerized plaques and tested at a strain rate of 1.3×10^{-3} s^{-1}. An Instron extensometer 2630-107 was used to collect accurate displacement data to measure the blend moduli. Two different impact tests were performed using test specimens prepared according to the ASTM D-256 protocol. The first test involved the standard Izod impact pendulum test and the second a fast tensile test (1 m/s) performed on a Zwick Rel SB 3122 tensile machine. In the latter test, the machined notches were sharpened prior to testing using a fresh razor blade, and the tensile toughness was defined as the ratio between the integrated force−displacement curve and the fracture surface area.

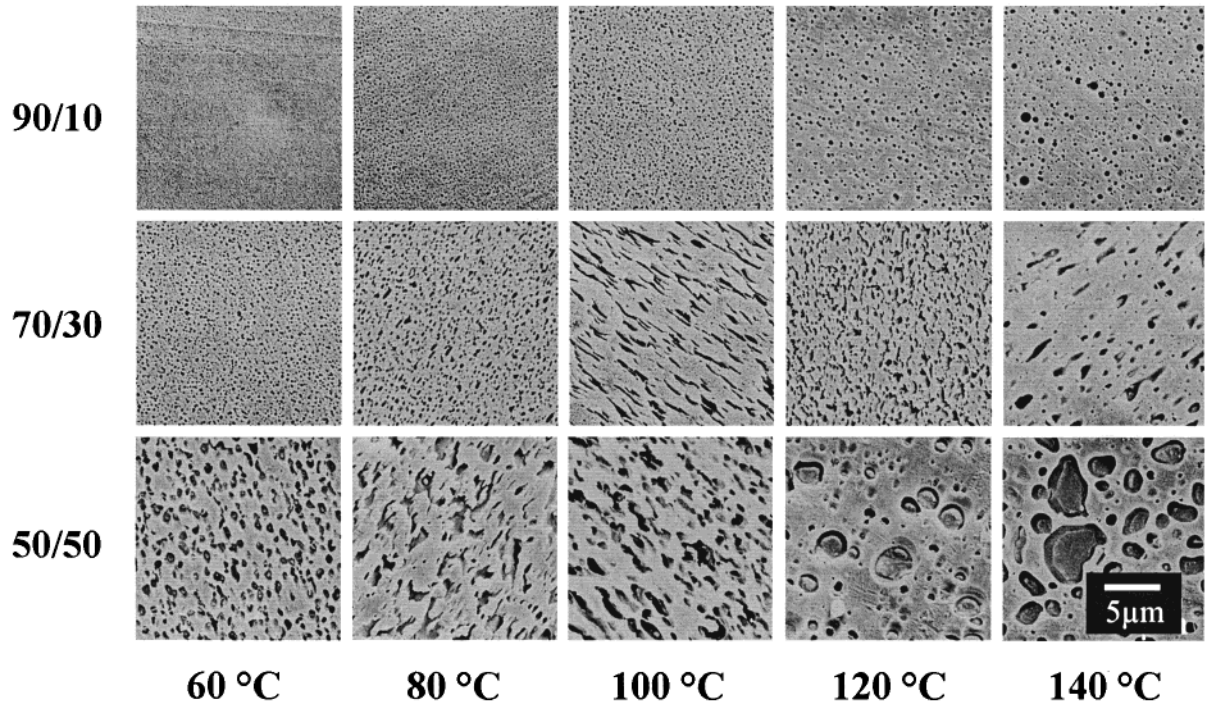

Figure 2. Morphology of PS/epoxy blends for three compositions cured at five different temperatures.

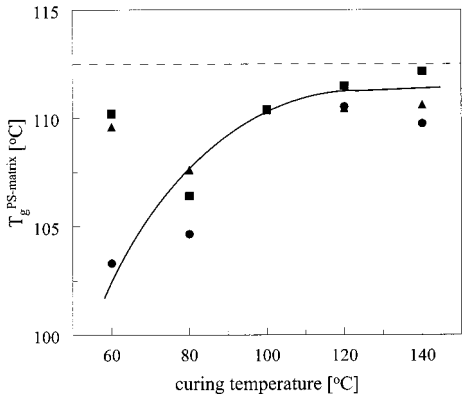

Figure 3. Glass transition temperatures of the PS matrix in PS/epoxy blends prepared by CIPS vs curing temperature: 90/10 (●),70/30 (▲), and 50/50 (■). The dashed line represents the T_g of neat PS.

3. Results and Discussion

3.1. Thermoplast/Epoxy Blends. 3.1.1. PS/Epoxy Blends. By controlling the coarsening process during chemically induced phase separation (CIPS) in thermoplast−epoxy systems, submicron or even nanosized morphologies could be produced.[21] In that introductory study an aromatic epoxy resin was used which yields a glassy, high-T_g, thermosetting dispersed epoxy phase. Here, an aliphatic epoxy resin (with PS as matrix phase) is used instead, and a rubbery phase is obtained, which might be used as a toughening agent (see Figure 2). Clearly, the particle size decreases with decreasing epoxy content and curing temperature, both suppressing coalescence. A disadvantage of lowering the curing temperature is the incomplete degree of demixing due to a suppressed phase separation given the high viscosity during morphology development. Figure 3 plots the resulting glass transition temperature, T_g, of the PS matrix vs curing temperature. The T_g depression of the (90/10) solution, cured at 60 °C, is larger than those for the (70/30) and (50/50) mixtures, where the morphology is the result of a thermally induced phase separation process (TIPS) occurring during cooling of the solutions prior to reaching the curing temperature of 60 °C. Apparently, TIPS results in higher T_g's for the blends than CIPS. The mechanical properties (strain to break and toughness) of all the PS/epoxy systems prepared were rather disappointing, due to the still too coarse morphologies obtained.

3.1.2. PMMA/Epoxy Blends. In contrast to PS/epoxy systems, PMMA/epoxy solutions are homogeneous over the whole composition range. Consequently, no TIPS occurs, and morphologies are the result of a CIPS process. More importantly, the critical ligament thickness of PMMA is larger than that of PS (thus experimentally more easy to obtain) and all solutions can be cured at the T_g of the initial solution, which is a requirement to produce submicron morphologies. In Figure 4, the morphologies of PMMA/epoxy 70/30 and 50/50 blends are shown as a function of curing temperature. For the 70/30 blend, the viscosity during phase separation (again) appears to be the morphology determining parameter since the size of the dispersed phase decreases with curing temperature. This eventually results in a transparent blend after curing at 60 °C, which corresponds to the T_g of the initial homogeneous solution. Despite its transparent appearance, the DMTA measurements in Figure 5a show the existence of a two-phase morphology; thus, the size of the dispersed phase has become too small to induce light scattering.[22] In contrast to the 70/30 system, the 50/50 system coarsens with decreasing curing temperature. An explanation can be found in the competition between the time scales involved in accomplishing phase separation and reaction. Considering the low solution viscosity for this composition, the final morphology is mainly determined by the effect of an enhanced reaction rate.[23] After phase separation, the morphology coarsening process due to coalescence is arrested by gelation and/or vitrification of one of the phases involved, and the particle size decreases at the enhanced reaction rates at the higher

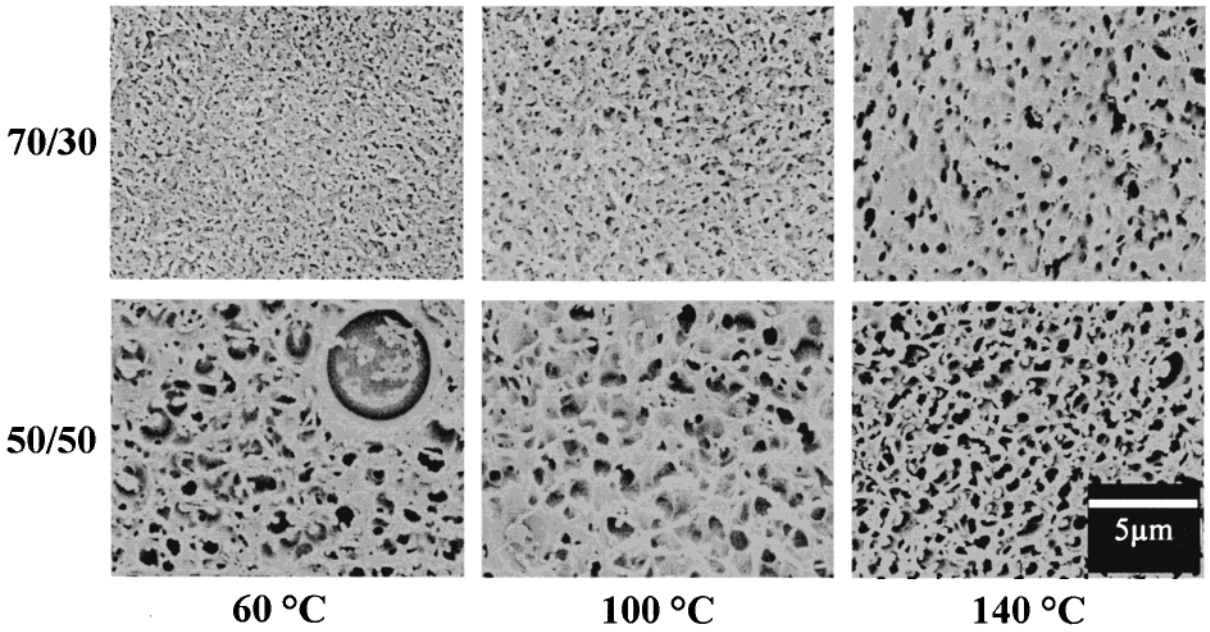

Figure 4. Morphology of PMMA/epoxy blends prepared by CIPS for a composition of 70/30 and 50/50 cured at 60, 100, and 140 °C.

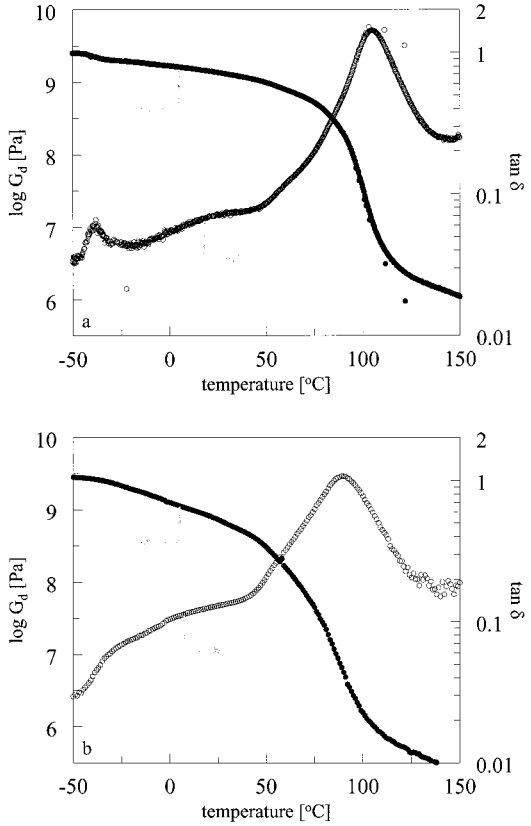

Figure 5. DMTA measurements of (transparent) PMMA/epoxy 70/30 blends cured at (a) 60 and (b) 220 °C.

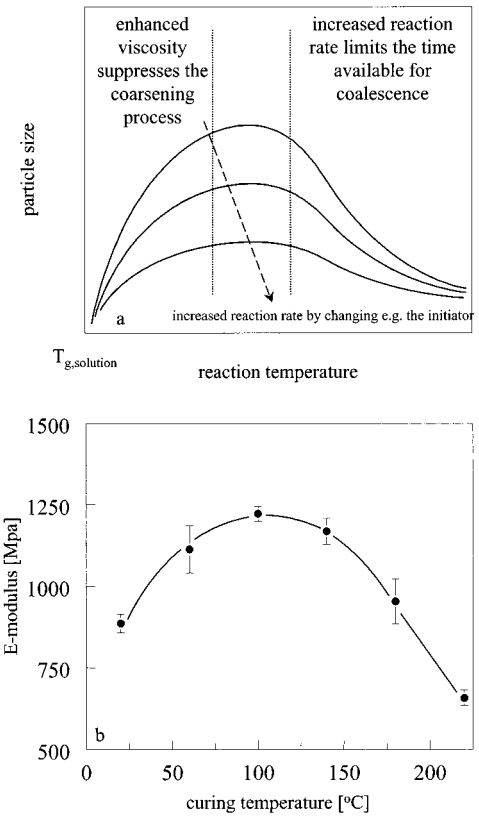

Figure 6. (a) Schematic presentation of the relation between the particle size and the curing temperature. (b) Modulus vs curing temperature for a PMMA/epoxy 60/40 system.

curing temperatures. Thus, a maximum is expected for the relation between particle size and curing temperature, as schematically depicted in Figure 6a. (This was confirmed by the PMMA/epoxy 70/30 system which showed small particles after curing at a temperature as high as 220 °C, not shown in Figure 4.) Though, an incomplete degree of demixing will be the main drawback of extreme curing conditions, at both high and low temperatures. The optimum in the modulus vs curing temperature of PMMA/epoxy 60/40 blends, as shown in Figure 6b, follows this reasoning. (Less plasticizing epoxy remains in the PMMA matrix if sufficient mobility and time are available for phase separation.) Incomplete demixing is also observed in the DMTA measurements of a PMMA/epoxy 70/30 solution cured at 220 °C (see Figure 5b). In contrast to the sample cured at 60 °C (see Figure 5a), the loss angle, tan δ, does no longer show two distinct peaks (for the epoxy and PMMA phase), and both transitions start to overlap and show peak

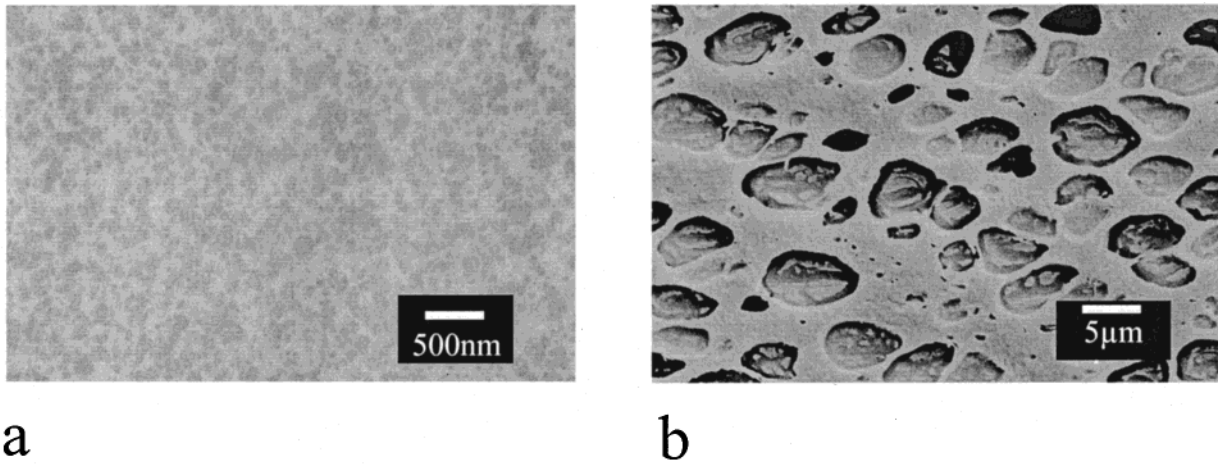

Figure 7. Morphology of in-situ polymerized PMMA/epoxy 50/50 blends, start temperature of polymerization profile: (a) 20 °C (TEM); (b) 60 °C (SEM).

Table 1. Relation between the Estimated Particle Size, *d* [μm], and the Strain at Break, ϵ_b [%], for Some PMMA/Epoxy Blends Cured at Different Temperatures

	90/10 PMMA/epoxy		70/30 PMMA/epoxy		50/50 PMMA/epoxy	
T_{cure} [°C]	d [μm]	ϵ_b [%]	d [μm]	ϵ_b [%]	d [μm]	ϵ_b [%]
60	0[a]	2.9	~0.05	27.4	2	3.9
100	0[a]	2.4	0.5	6.5	1.5	8.0
140	0[a]	2.0	1	2.8	1	48.2

[a] No separate rubber phase, homogeneous blend.

broadening which indicates an increased amount of interphase mixing.[24−26] For the same reason the dynamic modulus G_d gradually decreases over the broad temperature range between the T_g's of the neat polymers. (Another reason for the suppressed phase separation could be a possible reaction between PMMA and epoxy resin or curing agent.) Some interesting results concerning rubber toughening were obtained for the PMMA/epoxy 70/30 and 50/50 blends prepared via these routes. Table 1 demonstrates a distinct correlation between the particle size and the resulting strain at break. However, the blend preparation method and, consequently, the mechanical properties suffered from a relatively poor reproducibility. This may be improved by using a more advanced multistep processing route, e.g., in a proper mixer like a corotating twin-screw extruder,[27] but this possibility was not explored further since an interesting, relatively easy, alternative route exists: the MMA/epoxy systems.

3.2. Blends from in-Situ Polymerized MMA/Epoxy. 3.2.1. Polymerization. If, instead of PMMA, MMA monomer is used, a low viscous solution results consisting of MMA, epoxy resin, curing agent, and the radical initiators selected. MMA and epoxy are polymerized in situ by two noninterfering reactions: a free radical and a step-growth polymerization, respectively. This method is analogous to the classical routes used in the synthesis of interpenetrating polymer networks (IPNs).[28,29,37] The difference is that with IPNs crosslinking is used to suppress the coarsening process during phase separation,[37] while here we use an enhanced system viscosity since we aim at a continuous *thermoplastic* PMMA matrix.

Polymerization of MMA is started at room temperature in order to prepare a highly viscous gel, and therefore three different radical initiators are applied. To maximize the degree of phase separation and conversion of both polymerization reactions, the temperature is finally increased up to 120 °C, the T_g of pure PMMA[30] (see the Experimental Section). As an illustration, Figure 7 shows the resulting morphologies with the polymerization starting at 60 °C (low viscosity, Figure 7b) as compared to that starting at 20 °C (high viscosity, Figure 7a). In the second case, the particle size is decreased by an order of magnitude. Apart from incomplete demixing, a second drawback of controlling coarsening via viscosity is that it is more difficult to obtain full MMA conversion, especially for solutions with a higher epoxy concentration; see Figure 8 which shows the in-situ Raman conversion−time results. For 100% MMA, a stepwise increase in conversion is observed (Trommsdorf effect) because the enhanced viscosity during polymerization hinders the termination reactions more than the propagation reactions.[31] On dilution with 30% and 50% epoxy, the Trommsdorf effect becomes less pronounced, and a carefully designed polymerization schedule is more important in these cases.

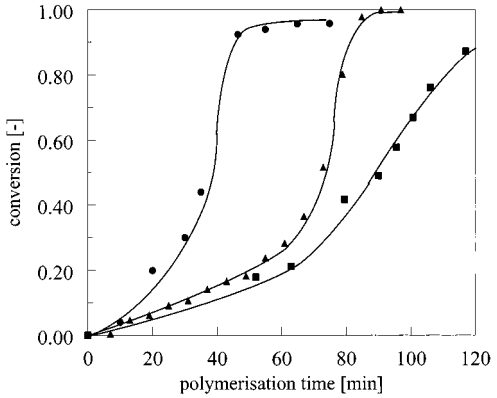

Figure 8. MMA conversion at 90 °C (1 mg of AIBN/g of MMA) measured by Raman spectroscopy vs the polymerization time, with epoxy resin as diluent: 0 (●), 30 (▲), and 50 wt % (■).

3.2.2. Morphology. The morphology of the in-situ polymerized blends is studied by solid-state NMR and transmission electron microscopy (TEM). The 50/50 blend has a hazy appearance, which is in accordance with the particle size observed of approximately 150 nm (see Figure 9d). Blends with a lower amount of epoxy are all transparent. In Table 2 the morphology sizes as determined via solid-state NMR by Mulder et al.[32] are presented. The size of the dispersed phase of PMMA/

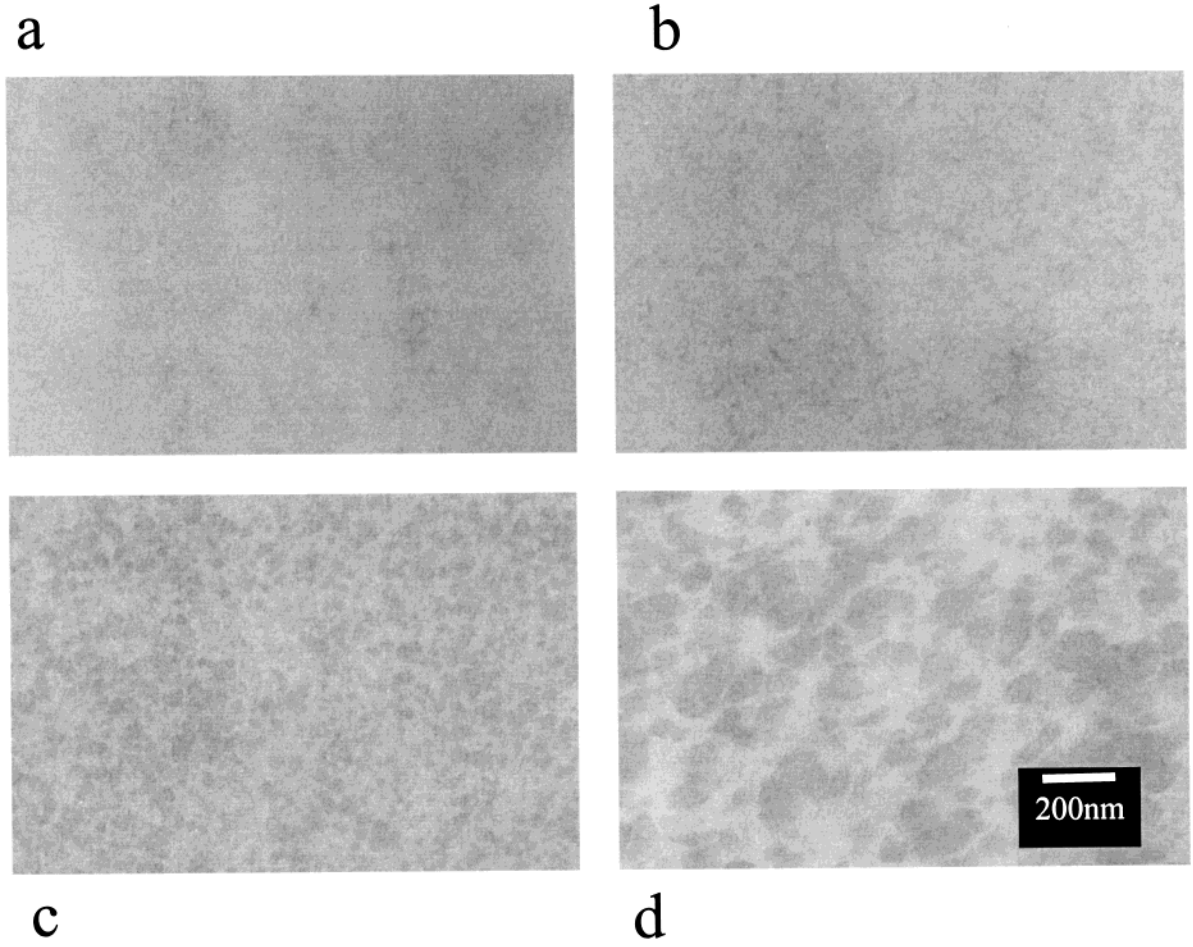

Figure 9. Transmission electron micrographs of the in-situ polymerized PMMA/epoxy blends: (a) 80/20, (b) 70/30, (c) 60/40, and (d) 50/50.

Table 2. Morphology Size of the Rubbery Epoxy Phase Determined Using Solid-State NMR[32]

PMMA/epoxy	domain size [nm]	PMMA/epoxy	domain size [nm]
90/10	0[a]	60/40	70
80/20	20	50/50	>100
70/30	30		

[a] Homogeneous.

epoxy 60/40 and 70/30 blend is receptively ~70 and ~30 nm, which is in accordance with the TEM micrographs shown in parts b and c of Figure 9. For the 80/20 blend, the dispersed phase is difficult to distinguish. According to the NMR study, phase separation has occurred in this system on a scale of approximately 20 nm. The 90/10 blend is homogeneous, and no evidence of phase separation is found using either of the techniques.

3.2.3. DMTA Measurements. Besides the morphology, also the composition of both phases is of importance for mechanical properties, and as a start, we focus on the 70/30 blend (which can be directly compared with the 70/30 PMMA/epoxy system of Figure 5). From the peak broadening in the loss angle (tan δ) (see Figure 10), the shoulder-like rubber transition, and the smooth decrease of the dynamic modulus (G_d) with increasing temperature, it can be concluded that, although phase separation has occurred, it seems to be partially incomplete. During in-situ polymerization of MMA/epoxy, PMMA formation is preceding that of the epoxy phase, but MMA conversion will not be complete until the final polymerization temperature, at the T_g of neat PMMA, is reached. As a result, there will always be some MMA present at all stages of the polymerization process, and especially after phase separation, the dispersed (cured) epoxy phase will be partially swollen with MMA which may be polymerized within this thermosetting network in a later stage. This obviously cannot occur in the PMMA/epoxy system of section 3.1 due to the absence of MMA monomer and explains the differences found[33] (compare Figures 5 and 10). Demixing is enhanced with increasing epoxy content (see Figure 10), and for the 50/50 and 30/70 blends clearly two tan δ peaks are observed, while for the homogeneous 90/10 system, as expected, only one tan δ peak is found.

3.2.4. Slow Speed Tensile Testing. In Figure 11 the tensile behavior of the in-situ polymerized MMA/epoxy system is shown, demonstrating a remarkable synergistic effect for the strain at break. While both neat polymers are rather brittle and the maximum network strain of PMMA is estimated to be ~75%,[9,34] strains of >100% are reached for the ductile blends of 70/30 to 30/70 compositions (homogeneous deformation, no macroscopic strain localization or stress whitening). Like neat PMMA, the 90/10 blend suffers from brittle fracture, while for the ductile 80/20 blend stress whitening is observed accompanied by strain localization and neck formation. (The microscopic deformation mechanisms in all blends have been studied by using in-situ small-angle X-ray scattering during tensile deformation.[35−37] Summarizing the results: the brittle 90/10 blend crazes while for higher epoxy contents shear yielding is observed. For the 80/20 blend shear yielding is preceded

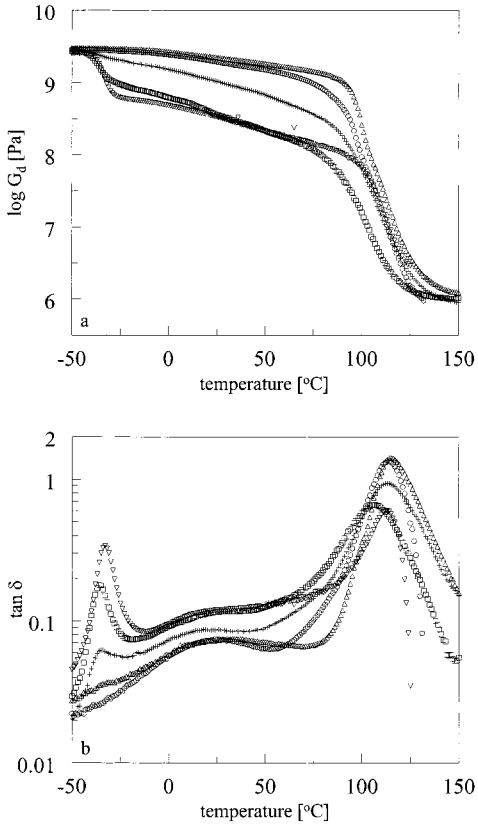

Figure 10. DMTA measurements of in-situ polymerized PMMA/epoxy blends: (a) dynamic modulus (G_d), (b) loss angle (tan δ). (△) 100/0, (○) 90/10, (+) 70/30, (□) 50/50, (▽) 30/70.

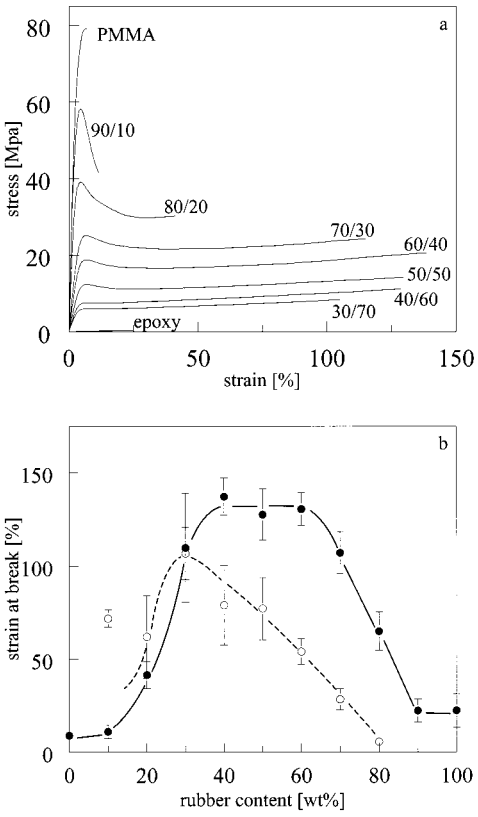

Figure 11. Tensile properties of the in-situ polymerized PMMA/epoxy blends: (a) stress−strain behavior; (b) macroscopic (●) and local (○) strain at break.

by cavitation, in contrast to the 70/30 and 50/50 blends where only a morphological orientation was observed.)

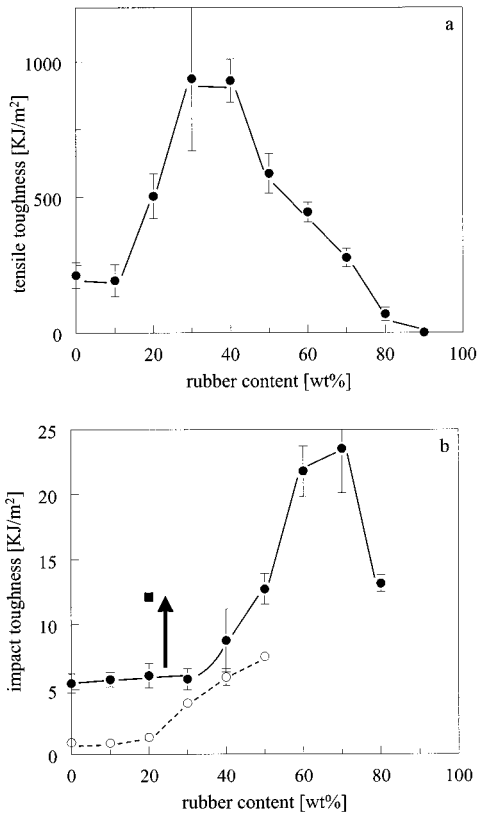

Figure 12. (a) Tensile toughness of the in-situ polymerized PMMA/epoxy blends. (b) Impact toughness of the same blends: (○) Izod test, (●) notched fast tensile test, (■) notched fast tensile test after predeformation in tension. Arrow shows jump in the impact toughness in the sample that has been predeformed.

The local strain at break in Figure 11b is determined by comparing the cross-sectional area of the test specimens before and after fracture (assuming the absence of dilatation processes, like crazing and rubber cavitation, during deformation) and reflects the amount of plastic deformation (the contribution of the PMMA network to the total macroscopic strain at break). The high macroscopic strain at break of the blends containing more than 40 wt % of epoxy seems to be a result of the enhanced influence of the elastic rubber phase, comparable to some PMMA-based IPNs where an enhanced strain at break was attributed to the tendency of the rubber phase to become continuous.[38−42] However, in our PMMA/epoxy systems, PMMA forms the continuous matrix up to a composition of 70 wt % epoxy, and the macroscopic properties found are partly due to the decreased ligament thickness of PMMA (which transforms the microscopic mode of deformation from crazing to shear yielding) and partly due to incomplete demixing; see the subsequent papers of this series, refs 35−37.

3.2.5. Tensile vs Impact Toughness. Figure 12 compares the tensile toughness (Figure 12a, definition see section 2.4) with the impact toughness (Figure 12b). The maximum in tensile toughness is obtained for 30−40 wt % epoxy as a result of the combination of a large strain at break and a relatively high yield stress and modulus. The maximum in impact toughness is observed at a significantly higher epoxy content, and all blends with epoxy content lower than 40 wt % are in fact brittle in impact (confirmed by the Izod impact results, the dashed line in Figure 12b). For Izod tests

the first improvement is found at a rubber content of 30 wt %, while for the notch tensile tests this value is shifted to 40 wt %. In the latter case the notch was sharpened prior to testing using a fresh razor blade which stresses the extreme notch sensitivity and thus the strain rate dependent toughness. Comparing the results of slow (Figure 12a) and fast (Figure 12b) testing with those of the time-resolved X-ray data,[35−37] we can conclude that at high deformation rates cavitation cannot occur, and therefore, brittle failure and poor impact toughness, equal to those of neat PMMA, are found. This absence of required cavitation during impact testing can be due to the strain rate dependence of the rubber modulus,[6,7] causing the modulus of the rubber phase to approach that of a glass, which prevents cavitation and thus the release of the local triaxial stress states that should precede massive shear yielding. To prove this, some samples of the 80/20 blend were predeformed in tensile at a relatively low deformation rate, to precavitate the samples, prior to notching and impact testing. This procedure resulted in a doubling of the impact toughness (see Figure 12b), finally yielding relative values comparable to the slow speed tensile toughness (see Figure 12a).

4. Conclusions

Two different blending routes, using chemically induced phase separation, were used to prepare rubber-modified PS and PMMA blends. In both cases, the morphology was tailored during the coarsening process after phase separation either by controlling either the system viscosity or the reaction rate. As a result, submicron or nanosized rubber morphologies were obtained that are principally interesting for toughening purposes of optically clear amorphous polymers. For in-situ polymerized MMA/epoxy systems a remarkable synergism in low-speed mechanical behavior is found, especially for the macroscopic strain at break. The tensile toughness starts improving at an epoxy content of 20 wt %; that is, however, still higher than the target value of <10 wt %. Insufficient phase separation caused the absence of the required heterogeneous systems at these low epoxy contents. At high deformation rates, almost all blends were brittle again, due to the inability to induce cavitation. The introduction of voids via slow-speed predeformation, prior to impact testing, was demonstrated for a PMMA/aliphatic-epoxy 80/20 composition;, this resulted in a significant increase in impact toughness. In conclusion, the results show that the toughness of brittle amorphous polymers can indeed be improved by the introduction of a submicron-sized dispersed rubber phase. However, the properties of this phase are important. It should be precavitated or easily cavitate at both low- and high-speed testing. To reach the ultimate toughness of low entangled polymers like PS, while keeping modulus and yield stress high by limiting the volume fraction of the dispersed phase to <10 wt %, further research should focus at obtaining a small (∼30 nm), well-distributed second phase of rather special core−shell particles with a relatively high modulus (30−300 MPa) rubbery shell and a low modulus core (≲3 MPa) which should easily cavitate even during fast deformation.[1−3,6,8] The refinement of the morphology, when scaled down to nanometer dimensions in rubber modified glassy polymer blends, can suppress the normal crazing response and can lead to quite tough behavior through ubiquitous rubber domain cavitation, followed by matrix ligament stretching. This has been also investigated in detail in past by Argon, Cohen, and co-workers in block copolymer blends of PS/PB.[43]

Acknowledgment. The authors thank T. Buijs, J. Ravenstijn, and I. van Casteren for their experimental contributions.

References and Notes

(1) Smit, R. J. M.; Brekelmans, W. A. M.; Meijer, H. E. H. *J. Mater. Sci.* **2000**, *35*, 2855.
(2) Smit, R. J. M.; Brekelmans, W. A. M.; Meijer, H. E. H. *J. Mater. Sci.* **2000**, *35*, 2869.
(3) Smit, R. J. M.; Brekelmans, W. A. M.; Meijer, H. E. H. *J. Mater. Sci.* **2000**, *35*, 2881.
(4) Bucknall, C. B. *Toughened Plastics*; Applied Science Publishers Ltd.: London, 1977.
(5) Riew, C. K.; Kinloch A. J. *Advances in Chemistry Series*; American Chemical Society: Washington, DC, 1993; Vol. 233.
(6) Smit, R. J. M.; Meijer, H. E. H.; Brekelmans, W. A. M.; Meijer H. E. H. *Comput. Methods Appl. Mech. Eng.* **1998**, *155*, 181.
(7) Smit, R. J. M. Ph.D. Thesis, Eindhoven University of Technology, 1998.
(8) Smit, R. J. M.; Brekelmans, W. A. M.; Meijer H. E. H. *J. Mech. Phys. Solids* **1999**, *47*, 201.
(9) Kramer, E. J.; Berger, L. L. *Adv. Polym. Sci.* **1990**, *91/92*, 1.
(10) Donald, A. M.; Kramer, E. J. *J. Polym. Sci., Polym. Phys. Ed.* **1982**, *20*, 899.
(11) Gent, A. N.; Thompkins, D. A. *J. Polym. Sci., Polym. Phys. Ed.* **1969**, *7*, 1483.
(12) Nariswa, I.; Yee, A. F. In *Crazing and Fracture in Polymers*; Thomas, E. L., Ed.; *Material Science and Technology*; VCH: Weinheim, 1993; Vol. 12, p 699.
(13) Hasan, O. A.; Boyce, M. C. *Polymer* **1993**, *34*, 24.
(14) Cross, A.; Haward, R. N. *Polymer* **1978**, *19*, 677.
(15) Govaert, L. E.; Melick van, H. G. H.; Meijer, H. E. H. *Polymer*, in press.
(16) Henkee, C. S.; Kramer, E. J. *J. Polym. Sci., Polym. Chem. Ed.* **1984**, *22*, 721.
(17) Sanden van der, M. C. M.; Buijs, L. G. C.; Bie de, F. O.; Meijer, H. E. H. *Polymer* **1994**, *35*, 2783.
(18) Sanden van der, M. C. M.; Meijer, H. E. H.; Lemstra, P. J. *Polymer* **1993**, *34*, 2148.
(19) Venderbosch, R. W.; Meijer, H. E. H.; Lemstra, P. J. *Polymer* **1994**, *33*, 4349.
(20) Venderbosch, R. W.; Meijer, H. E. H.; Lemstra, P. J. *Polymer* **1995**, *36*, 2903.
(21) Jansen, B. J. P.; Meijer, H. E. H.; Lemstra, P. J. *Polymer* **1999**, *40*, 2917.
(22) Conaghan, B. F.; Rosen, S. L. *Polym. Eng. Sci.* **1972**, *12*, 134.
(23) Yamanaka, K.; Takagi, Y.; Inoue, T. *Polymer* **1989**, *60*, 1839.
(24) Lipatov, Y. S. In *Advances in Chemistry Series*; Klempner, D., Sperling, L. H., Utracki, L. A., Eds.; American Chemical Society: Washington, DC, 1994; Vol. 239, p 125.
(25) Hourston, D. J.; Schäfer, F. U. In *IPNs Around the World*; Kim, S. C., Sperling, L. H., Eds.; John Wiley & Sons: Chichester, 1997; p 155.
(26) Akay, M.; Rollins, S. N. *Polymer* **1993**, *34*, 967.
(27) Nelissen, H.; Pas, R. European Patent, EP-A1-0720901. Kok de, J. M. M. Internal Report, Eindhoven University of Technology, 1997.
(28) Klempner, D.; Sperling, L. H.; Utracki, L. A. *Advanced Chemistry Series*; American Chemical Society: Washington, DC, 1994; Vol. 239.
(29) Kim, S. C.; Sperling, L. H. *IPNs Around the World*; John Wiley & Sons: Chichester, 1997.
(30) Kim, S.; An, J. H. *J. Appl. Polym. Sci.* **1995**, *58*, 491.
(31) Trommsdorff, E. *Makromol. Chem.* **1970**, *1*, 169.
(32) Mulder, F. M.; Jansen, B. J. P.; Lemstra, P. J.; Meijer, H. E. H.; Groot de, H. J. M. *Macromolecules* **2000**, *33*, 457.
(33) Mishra, V.; Du Prez, F. E.; Goethals, E. J.; Sperling, L. H. *J. Appl. Polym. Sci.* **1995**, *58*, 347.
(34) Donald, A. M.; Kramer, E. J. *J. Polym. Sci., Polym. Phys. Ed.* **1982**, *20*, 899.
(35) Jansen, B. J. P.; Rastogi, S.; Meijer, H. E. H.; Lemstra, P. J. *Macromolecules* **2001**, *34*, 4007−4018.

(36) Jansen, B. J. P.; Rastogi, S.; Meijer, H. E. H.; Lemstra, P. J. *Macromolecules* **1999**, *32*, 6283.
(37) Jansen, B. J. P.; Rastogi, S.; Meijer, H. E. H.; Lemstra, P. J. *Macromolecules* **1999**, *32*, 6290.
(38) Akay, M.; Rollins, S. N. *Polymer* **1993**, *34*, 1865.
(39) Akay, M.; Rollins, S. N.; Riordan, E. *Polymer* **1988**, *29*, 37.
(40) Han, X.; Chen, B.; Guo, F. In *IPNs Around the World*; Kim, S. C., Sperling, L. H., Eds.; John Wiley & Sons: Chichester, 1997; p 241.
(41) Gilmer, T. C.; Hall, P. K.; Ehrenfeld, H.; Wilson, K.; Bivens, T.; Clay, D.; Endreszl, C. *J. Polym. Sci., Polym. Phys.* **1996**, *34*, 1025.
(42) Kojima, T.; Ohnaga, T.; Inoue, T. *Polymer* **1995**, *36*, 2197.
(43) Argon, A. S.; Cohen, R. E.; Gebizlioglu, O. S.; Schwier, C. E. In *Advances in Polymer Science;* Kausch, H. H., Ed.; Springer-Verlag: Berlin, 1983; Vol. 52/53, p 275.

MA001809Z